

Generation of Active Sites for CO Photooxidation on TiO₂ by Platinum DepositionHisahiro Einaga,^{*,†} Masafumi Harada,[‡] Shigeru Futamura,[†] and Takashi Ibusuki[†]

National Institute of Advanced Industrial Science and Technology, AIST Tsukuba West, 16-1 Onogawa, Tsukuba, Ibaraki 305-8569, Japan, and Department of Textile and Apparel Science, Faculty of Human Life and Environment, Nara Women's University, Nara 630-8506, Japan

Received: February 12, 2003; In Final Form: June 9, 2003

Photocatalytic oxidation of CO to CO₂ was carried out with TiO₂ and Pt/TiO₂ catalysts at room temperature to investigate the effect of Pt deposition. The rate for CO photooxidation by Pt/TiO₂ was higher than that by TiO₂. The reaction rate increased with incident light intensity to the power of 0.7 for Pt/TiO₂ and 0.5 for TiO₂. The dependency of reaction rate on the concentration of CO and water vapor was explained in terms of Langmuir–Hinshelwood mechanism, where CO was more efficiently adsorbed on Pt sites compared with TiO₂. On the basis of diffuse reflectance FTIR spectroscopic studies and CO photodesorption measurements, Pt on TiO₂ acted as the active sites on which CO was chemically adsorbed and oxidized to CO₂ on photoirradiation in the presence of O₂.

Introduction

Photocatalytic oxidation with semiconductor metal oxides has attracted much interest in recent decades since it is useful for the transformation and decomposition of organic compounds under mild conditions.^{1–5} In the photooxidation reactions with TiO₂ catalyst, highly reactive electron–hole pairs are generated on the metal oxide by absorbing incident photons that have an energy larger than the band gap of TiO₂. In the presence of O₂, various types of active oxygen species are formed on the catalyst surface,^{6,7} and they oxidize the substrates adsorbed on the catalyst surface. Hitherto, TiO₂-catalyzed photoreactions have been applied to the purification of water and air polluted with hazardous compounds. Therefore, it is desired to obtain information on chemical events on photoirradiated TiO₂ in detail from the standpoint of not only fundamental research but also practical utilization.

Doping of transition metals to TiO₂ has been extensively studied since they produce the longer electron–hole pair separation.^{8,9} Especially, Pt-deposited TiO₂ (Pt/TiO₂) has been frequently used for photoreactions and reported to enhance the rate for the splitting of water,^{10,11} hydrogen generation from alcohol–water solution,^{12,13} and oxidation of organic compounds.^{14–16} It has been reported, however, that the metal doping has also a negative effect on the photoreaction depending on conditions.¹⁷

We have investigated the photooxidation of gaseous benzene in air over TiO₂ and metal-doped TiO₂ catalysts.¹⁸ Benzene was completely oxidized to CO₂ on the photoirradiated Pt/TiO₂ catalyst without CO formation in humid air at room temperature.¹⁸ In this reaction, benzene was decomposed to CO₂ and CO, and the byproduct CO was subsequently oxidized to CO₂ on the catalyst. Deposition of Pt on TiO₂ greatly enhanced the CO oxidation rate, while pure TiO₂ did not show the activity for CO photooxidation under highly humidified conditions.

Enhancement of CO oxidation rate by Pt deposition on TiO₂ has been reported by several groups. Vorontsov et al. performed the photooxidation reaction (CO concentration = 5000 ppm) in air at 313 K using the 0.4 wt % Pt/TiO₂ catalyst prepared by the photodeposition method.¹⁹ They reported that the quantum yield for the photooxidation by Pt/TiO₂ was about 17 times higher than that by TiO₂. Takahama et al. prepared TiO₂/pillared montmorillonite clay catalysts and used them for the CO photooxidation (CO concentration = 50 ppm) at room temperature.²⁰ They found that a Pt-deposited catalyst showed 80% of CO conversion at the space velocity of 9000 h^{−1}, while the catalyst without Pt showed almost no activity under the same conditions. Thus, the Pt deposition is effective for the reaction at around room temperature.

On the other hand, Linsebigler et al. investigated the photodesorption of CO chemisorbed on TiO₂(110) single crystal at 105 K where thermally activated reactions were quenched.²¹ The initial CO₂ formation rate and CO₂ yield decreased by deposition of Pt on the TiO₂ surface. They reported that Pt deposited on TiO₂ was ineffective in the CO photooxidation under the conditions where the thermal reactions were quenched. The results indicated that the deposited Pt was not involved in the electronic excitation processes. They suggested that the negative effect of Pt on the CO₂ yield was due to its nucleation on defect sites, which reduced the number of chemisorbed O₂ molecules available for the CO photooxidation. Thus, the effect of Pt deposition on the CO photooxidation strongly depends on the reaction conditions.

These findings urged us to clarify the mechanism for the CO photooxidation with Pt/TiO₂. In contrast with the CO oxidation on single-crystal Pt surface performed at low pressure,²² only a few papers have been reported on the CO photooxidation on Pt/TiO₂, and the role of Pt in the reaction has not been clarified yet. In this study, photocatalytic oxidation of CO to CO₂ over TiO₂ and Pt/TiO₂ catalysts was carried out at room temperature and the reaction mechanism was investigated by means of kinetic analysis, diffuse reflectance FTIR studies, and CO photodesorption measurements. The objective of this study is to show how the Pt deposition enhances the CO photooxidation

* To whom correspondence should be addressed. E-mail: h-einaga@aist.go.jp.

[†] National Institute of Advanced Industrial Science and Technology (AIST).

[‡] Nara Women's University.

rate under ambient conditions. Our findings suggest that adsorption of CO onto catalyst surface is one of the key steps for the CO photooxidation at room temperature and the efficient adsorption of CO on the Pt sites contributes to the enhanced CO oxidation rate.

Experimental Section

Catalysts. Commercially available TiO₂ (P25; Japan Aerosol Co. Ltd.) was used as catalyst and precursor. The BET surface area was 43 m²/g. Pt was deposited on TiO₂ at the loading of 1.0 wt % by the photodeposition method. TiO₂ (0.5 g) was dispersed into the ethanol (150 mL)–water (100 mL) solution containing 2.56×10^{-5} mol of H₂PtCl₆·6H₂O in a Pyrex glass vessel with vigorous stirring. After N₂ gas was bubbled into the suspension for 30 min to remove the dissolved O₂, it was photoirradiated by a 500 W high-pressure Hg lamp for 3 h with continuous stirring. The suspension was then filtered off, washed with water, and dried at 383 K. It was confirmed by the analysis of the filtrate on ICP (Thermo Jarrell Ash Co. IRIS/AP) that more than 99.9% of Pt was removed from the ethanol–water solution. Datye et al. pointed out that some Pt was deposited on the glass during the photodeposition.²³ In this work, however, the Pt loading was conveniently estimated by the amount of the precursor Pt complex and TiO₂.

Characterization of Pt Particles on TiO₂. Transmission electron micrographs (TEM) of the Pt particles on TiO₂ were taken using a JEOL-200CX electron microscope at accelerating voltage of 200 kV. The catalyst was mixed with water, and the water suspension of catalyst was ultrasonicated for several minutes. After ultrasonication, a drop of this suspension was deposited on a carbon film-coated copper grid and then dried completely in ambient air.

For EXAFS measurements of the Pt-L₃ edge of the catalyst of Pt particles on TiO₂, the catalyst sample was pressed to make a self-supporting disk with appropriate optical thickness. The EXAFS measurements were performed in transmission mode at room temperature, using the beam line 10B, at the Photon Factory of the High Energy Accelerator Research Organization (KEK-PF).

In the EXAFS analysis described in detail elsewhere,^{24,25} the raw EXAFS data in energy space ($\ln(I_0/I)$ vs E) were reduced to the photoelectron wave vector (k) space, where $k = [2m(E - E_0)/\hbar^2]^{1/2}$, with the threshold energy E_0 . The $k^3\chi(k)$ functions vs k data and the corresponding Fourier transforms were obtained using a Hanning window function with 1/10 of the FT ranges. The Fourier transformation from k space to r space was 40–160 nm⁻¹. For the curve fitting, the high-frequency noise was removed by a Fourier filtering, and the inverse Fourier transformation to k space (the range 50–150 nm⁻¹) was employed.

$$k^3\chi(k) = \sum_j N_j F_j(k_j) k_j^2 \exp(-2\sigma_j^2 k_j^2) \sin[2k_j r_j + \phi_j(k_j)] / r_j^2 \quad (1)$$

$$k_j = (k^2 - 2m\Delta E_{0j}/\hbar^2)^{1/2} \quad (2)$$

where N_j , r_j , ΔE_{0j} , σ_j , $F_j(k_j)$, and $\phi_j(k_j)$ represent the coordination number, the bond distance, the difference between the theoretical and experimental threshold energies, the Debye–Waller factor, the backscattering amplitude function, and phase shift function of the j th coordination shell. The resulting filtered data were fitted, with the backscattering amplitude $F_j(k_j)$ and the phase shift $\phi_j(k_j)$ functions derived from the reference compound (Pt foil in this experiment), to obtain detailed structural information.

Apparatus for Photocatalytic Measurements. Photoreactions were carried out with a flow-type reactor. The reactor was fabricated from a Pyrex glass tube with a quartz glass window and contained a square-shaped glass plate (50 mm × 45 mm). The catalyst was coated on one side of the glass plate from an aqueous slurry of catalyst powder and dried at 383 K. Photoirradiation was carried out for the catalyst through the quartz glass window by a 500 W high-pressure Hg lamp equipped with a band path filter (365 nm). The numbers of photons were counted by potassium ferrioxalate actinometry according to the literature method.²⁶ The light intensity was changed by using the sheets of polyethylene–terephthalate film.

Reaction gases were prepared by mixing 1% CO (air balance; Takachiho Kogyo Co. Ltd.) or 500 ppm CO (N₂ balance) with N₂ (99.99%, total hydrocarbon < 1 ppm) and O₂ (99.99%, total hydrocarbon < 1 ppm). All the reactions were carried out at the O₂ concentration of 20%. When reactions were carried out under humidified conditions, water vapor was introduced to reaction gases by passing N₂ through a water bubbler. The reaction temperature was around 295 K.

As a pretreatment, the catalyst was photoirradiated in air to decompose the organic impurities adsorbed on TiO₂ surface. After the gas–solid adsorption equilibrium of the substrate was achieved in the reactor, photoirradiation was started. Concentrations of CO₂ and CO were simultaneously determined by a gas chromatograph (GL Sciences GC-390B) equipped with a thermal conductivity detector (TCD), a flame ionization detector (FID), and a methane converter. The CO photooxidation rates (denoted by R) was calculated according to eq 3, where X , C_0 , F , and W denote conversion of CO, the inlet concentration of benzene, the flow rate of CO, and the catalyst weight, respectively. Reaction rates were measured under the conditions where the conversions were lower than 15% and the reactions reached the stationary state.

$$R = XC_0F/W \quad (3)$$

Catalyst weight on the plate was 7.5 mg (±0.3 mg), and the averaged catalyst weight was around 0.3 mg/cm². At this loading level, the reaction rate linearly depended on the catalyst weight, indicating that the catalyst on the plate was fully photoirradiated. In general, the rate of the photocatalytic reaction with TiO₂ is dominated by the surface reaction on the catalyst or mass transfer process in the reactor.²⁷ In this study, the kinetic measurements were carried out with flow rate at 50–100 mL/min, where the reaction rate did not depend on the flow rate. Therefore, mass transfer process was not reflected in the apparent reaction rates.

Diffuse Reflectance FTIR Spectroscopic Study. FTIR spectra of catalysts were measured on a JASCO FT/IR-480 Plus spectrometer with a TGS detector and a diffuse reflectance accessory (DR-81). The accessory was enclosed with a cubic cell fabricated from acryl resin (cell volume: ca. 2250 mL). The cell had a quartz glass window on its upper site and a set of connectors to allow reaction gases to flow through the cell. A 500 W high-pressure Hg lamp equipped with a 365 nm band path filter was used as the light source. Freshly prepared Pt/TiO₂ samples or TiO₂ samples were placed in the diffuse reflectance accessory. The catalyst sample was photoirradiated through the quartz window. Flow rate of reaction gas was set at 500 mL/min. It took about 12 min to purge the cell completely. Prior to the FTIR measurements, the catalyst sample was photoirradiated in humidified air. After the background spectra were taken without the feed of CO in the dark, the reaction gas containing 2.03×10^{-5} mol/L of CO was

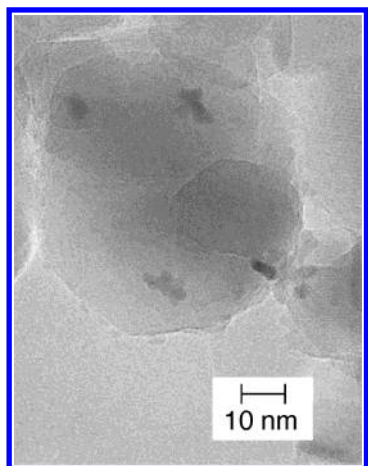


Figure 1. Transmission electron micrograph of Pt particles supported on TiO₂ prepared by the photodeposition method at 1 wt % metallic weight.

introduced into the cell. Photoirradiation was started, and the spectra were taken after the cell was completely filled with the reaction gas.

Photodesorption Measurement of CO. Details of the reactor used for photodesorption of CO on catalysts have been described elsewhere.^{18,28} The reactor was composed of an inner glass rod (8 mm outer diameter, 500 mm length) and an outer glass tube (13 mm inner diameter). The surface area of the inner rod was around 125 cm². The reactor was photoirradiated by four 20 W black lights (TOSHIBA FL20S-BLB-A). The emitted light from the lamp distributed in the wavelength range 300–420 nm with a maximum intensity at 356 nm. Catalyst sample was coated on the surface of the inner rod from the aqueous suspension and dried at 383 K. The catalyst weight was 52.5 mg (averaged catalyst weight: 0.4 mg/cm²). It was confirmed that the catalyst on the reactor was fully photoirradiated at this loading level.¹⁸ The volume of the reaction vessel was approximately 42 mL, and it took about 120 s to purge the vessel completely by the 50 mL/min of gas flow. Gas samples were analyzed on a differentially pumped quadrupole mass spectrometer MicroVision Plus 200D (Spectra International). ¹³C-labeled CO was used instead of ¹²CO in this experiment to avoid the overlap of its signal with the large background signal of ¹⁴N₂.

Results and Discussion

Characterization of Pt Particles on TiO₂. Figure 1 shows the TEM image of Pt particles on TiO₂. The larger particles with a size of about 70 nm are assigned to be TiO₂ particles, in comparison of TEM image of original TiO₂ powder without Pt particles. The Pt particles deposited on TiO₂ are distributed over the whole TiO₂ surface. The size of Pt particles is found to be 2–3 nm in diameter.

Figure 2 shows the Fourier transforms of the EXAFS data for the catalyst sample of Pt particles on TiO₂ and Pt foil (reference compound). The main peaks around 0.275 nm of both the compounds are assigned to the Pt–Pt bond. The main peak is lower for the catalyst sample than for Pt foil, due to the decrease of coordination number of Pt atoms around the Pt atom on the TiO₂ catalyst. The data for the catalyst sample were then Fourier-filtered over 0.20–0.30 nm and were fit to a one-shell of Pt–Pt bond, using $F_j(k_j)$ and $\phi_j(k_j)$ functions derived from the Pt foil, to get some structural parameters (coordination number, bond distance, Debye–Waller factor, etc.) of the catalyst sample. For this sample, the coordination number, the bond distance, and Debye–Waller factor are 9.0, 0.276 nm, and

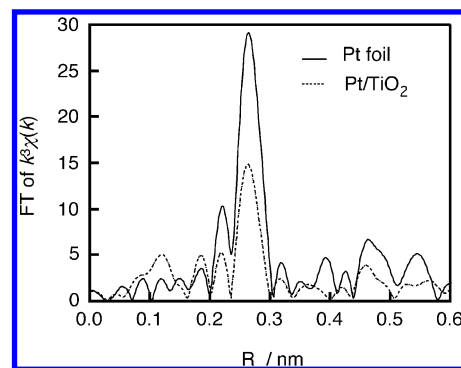


Figure 2. Fourier transforms over $k = 40\text{--}160\text{ nm}^{-1}$ of the k^3 -weighted EXAFS data of the Pt L₃-edge for catalyst sample and Pt foil.

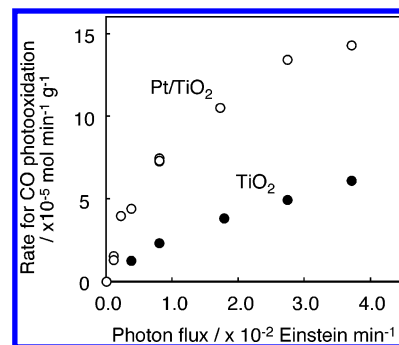


Figure 3. Effect of incident light intensity on the rate for CO photooxidation over TiO₂ and Pt/TiO₂ without water vapor. Light source: 500 W high-pressure Hg lamp with 365 nm band path filter. CO concentration: 4.03×10^{-4} mol/L.

3.93×10^{-2} nm, respectively. Here, the average diameter estimated from this coordination number is 2.0 ± 0.2 nm, assuming the spherical particle and fcc structure of the obtained Pt particles. This value is as the same as the particle size diameter (2–3 nm) from the TEM image (Figure 1).

Kinetics for CO Photooxidation. Figure 3 shows the effect of incident light intensity on the rate of CO photooxidation with TiO₂ and Pt/TiO₂ catalysts ($[\text{CO}] = 4.03 \times 10^{-4}$ mol/L, $[\text{O}_2] = 20\%$, $[\text{H}_2\text{O}] = 0\%$). The CO photooxidation rate monotonically increases with the light intensity and is enhanced by deposition of Pt on TiO₂. It has been reported that the relationship between the intensity of incident light (I) and the reaction rate (R) can be expressed by eqs 4 and 5.^{29–33} Here, k is the observed rate constant and α is a constant.

$$R = k(I)^\alpha \quad (4)$$

$$\log R = \alpha \log(I) \quad (5)$$

Figure 4 shows log–log plots of the CO photooxidation rate versus photon flux in the region higher than 0.377×10^{-2} einstein min^{−1} of photon flux. Good linear relationships are observed for both TiO₂ and Pt/TiO₂ catalysts. From the value of the slopes, α is estimated to be 0.5 for Pt/TiO₂ and 0.7 for TiO₂, respectively.³⁴ According to the simplified equations described by Egerton and King, the reaction rate of photooxidation reactions on TiO₂ is proportional to incident light intensity in the low-intensity region and to square-root of light intensity in the high-intensity region.³⁵ In the former case, formation of electron–hole pair is the rate-determining step. In the latter case, on the other hand, the reaction of hole to form the active oxygen species responsible for CO oxidation is the rate-determining step. In the TiO₂-catalyzed photooxidation of 2-propanol, formic acid, and acetone, the α values have been in the range of 0.5 to

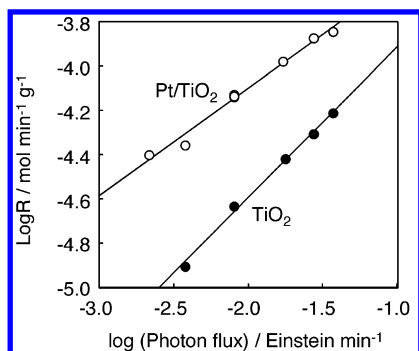


Figure 4. log–log plots for incident light intensity and the rate for CO photooxidation. Light source: 500 W high-pressure Hg lamp with 365 nm band path filter. CO concentration: 4.03×10^{-4} mol/L.

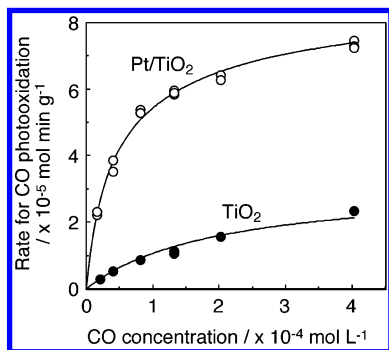


Figure 5. Effect of the CO concentration on the rate for CO photooxidation over TiO₂ and Pt/TiO₂ without water vapor. Incident light intensity at 365 nm: 7.0 mW. The solid lines are the calculated data by using the values of K and k evaluated from the Langmuir–Hinshelwood equation (see text).

0.7.^{29–33} The α values for the CO oxidation obtained in this study also fall in this range. The deviation from the value 0.5 and 1.0 implies that the reaction is in the transition states between the two regions. As noted above, the catalysts were photoirradiated in the humidified air as the pretreatment. We have reported that CO is oxidized to CO₂ on Pt/TiO₂ catalyst in the dark after the catalyst is photoirradiated in humid air.³⁶ However, the catalyst was gradually deactivated without continuous photoirradiation and the CO oxidation rate was below 10^{-6} mol min⁻¹ g⁻¹ at the stationary state. It has been reported that CO is oxidized to CO₂ on the single-crystal Pt surface at a low pressure (typically total pressure is lower than 10^{-4} Torr) without photoirradiation.²² In this reaction, O₂ is adsorbed on Pt to form oxygen atom, which oxidizes CO to CO₂. With a high concentration of CO at ambient temperature, Pt on TiO₂ is generally inactive or has a poor activity for CO oxidation without photoirradiation. It has been reported that, under these conditions, CO is strongly adsorbed on Pt metal and inhibits the dissociative adsorption of O₂ that is necessary for CO oxidation even under conditions of moderate CO surface coverage.³⁷

Figure 5 shows the effect of the CO concentration on the rate of CO photooxidation (photon flux 0.800×10^{-2} einstein min⁻¹, [O₂] = 20%, [H₂O] = 0%). The photooxidation rates increase with increasing the CO concentration for both catalysts. The increment for Pt/TiO₂ catalyst is much larger than that for TiO₂ catalyst in the low-concentration region. The rates are almost saturated in the higher concentration region. This dependency on the concentration of substrate has been generally observed for the TiO₂-catalyzed photooxidation of organic compounds in the aqueous phase and in gas phase.^{9,11,38} It has been reported that the photoreaction proceeds via the Langmuir–

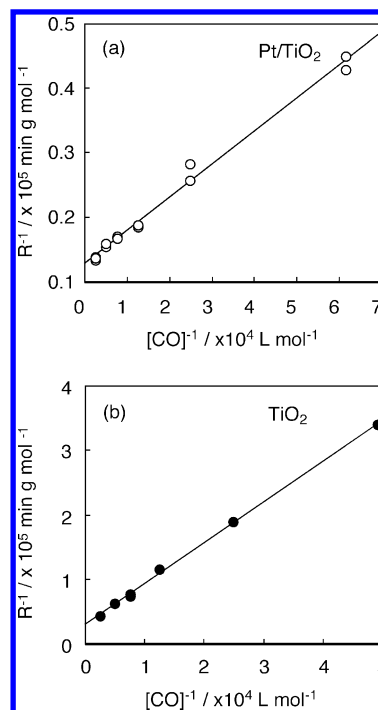


Figure 6. Reciprocal plots for the CO concentration and the rate for CO photooxidation. Incident light intensity at 365 nm: 7.0 mW.

Hinshelwood (abbreviated as L–H) type mechanism,^{38–41} where the substrate is preadsorbed on TiO₂ surface prior to the photoreaction. According to the L–H type mechanism, the reaction rate (R) can be expressed as eq 6 for TiO₂ catalyst, where K_{TiO_2} refers to the equilibrium constant for CO adsorption on TiO₂ surface, k_{TiO_2} the rate constant for the oxidation of adsorbed CO on TiO₂ surface, and $[\text{CO}]$ the CO concentration, respectively:⁴²

$$R = \frac{k_{\text{TiO}_2} K_{\text{TiO}_2} [\text{CO}]}{1 + K_{\text{TiO}_2} [\text{CO}]} \quad (6)$$

For Pt/TiO₂ catalyst, reaction rate can be expressed as eq 7, since CO can also be adsorbed on Pt and oxidized to CO₂, as discussed later:⁴²

$$R = \frac{k_{\text{TiO}_2} K_{\text{TiO}_2} [\text{CO}]}{1 + K_{\text{TiO}_2} [\text{CO}]} + \frac{k_{\text{Pt}} K_{\text{Pt}} [\text{CO}]}{1 + K_{\text{Pt}} [\text{CO}]} \quad (7)$$

Here, K_{Pt} is the equilibrium constant for CO adsorption on active sites on Pt and k_{Pt} the rate constant for the oxidation of adsorbed CO on Pt. Figure 6 shows the reciprocal plots for the dependence of reaction rate on the CO concentration. In the L–H kinetic equations (6) and (7), the reciprocal plots show linear correlations. Numerical values are obtained from the reciprocal plots and summarized in Table 1.⁴³ From the numerical values, the reaction rates are calculated and compared in Figure 5. The experimental data agree well with the calculated data, supporting the above kinetics. The value of the equilibrium constant for Pt/TiO₂ is 7 times larger than that for TiO₂. As definitions, θ_{TiO_2} and θ_{Pt} are the fractions of active sites on TiO₂ and Pt that are covered with CO (eqs 8 and 9). They can be calculated from the values of the equilibrium constants and are summarized in Table 2. The value of θ_{Pt} is larger than that of θ_{TiO_2} especially in the low concentration of CO. The increase in the fraction of active sites increases the photooxidation rate. It is worth noting that the rate constant k_{Pt} is about 1.76 times

TABLE 1: Kinetic Parameters

K_{TiO_2}	$4.94 \times 10^3 \text{ L mol}^{-1}$	K_{Pt}	$3.47 \times 10^4 \text{ L mol}^{-1}$
k_{TiO_2}	$3.19 \times 10^{-5} \text{ mol min}^{-1} (\text{g of catal})^{-1}$	k_{Pt}	$5.64 \times 10^{-5} \text{ mol min}^{-1} (\text{g of catal})^{-1}$
$K_{\text{TiO}_2}^{\text{in}}$	$6.26 \times 10^4 \text{ L mol}^{-1}$	$K_{\text{Pt}}^{\text{in}}$	$1.66 \times 10^4 \text{ L mol}^{-1}$

TABLE 2: Fraction of Surface Covered with CO (θ)

CO concn (mol L^{-1})	θ	
	Pt	TiO ₂
2.03×10^{-6}	0.066	0.010
4.06×10^{-6}	0.123	0.020
2.03×10^{-5}	0.413	0.091
4.06×10^{-5}	0.585	0.167

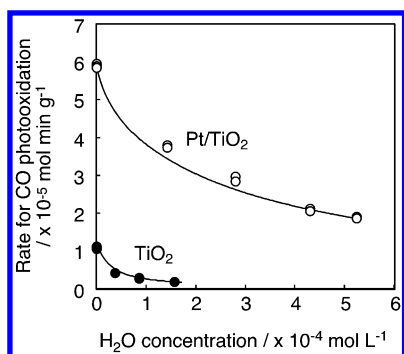


Figure 7. Effect of the concentration of water vapor on the rate for CO photooxidation over TiO₂ and Pt/TiO₂. Incident light intensity at 365 nm: 7.0 mW. CO concentration: $1.32 \times 10^{-4} \text{ mol/L}$. The solid lines are the calculated data by using the value of K' evaluated from the Langmuir–Hinshelwood equation (see text).

larger than k_{TiO_2} . This indicates that the oxidation rate of adsorbed CO on the Pt sites is higher than that on TiO₂ surface.

$$\theta_{\text{TiO}_2} = \frac{K_{\text{TiO}_2}[\text{CO}]}{1 + K_{\text{TiO}_2}[\text{CO}]} \quad (8)$$

$$\theta_{\text{Pt}} = \frac{K_{\text{Pt}}[\text{CO}]}{1 + K_{\text{Pt}}[\text{CO}]} \quad (9)$$

We have reported that the rate of CO photooxidation strongly depends on the concentration of water vapor.¹⁸ Figure 7 shows the dependence of CO photooxidation rate on the concentration of water vapor in the reaction gas (photon flux $0.800 \times 10^{-2} \text{ einstein min}^{-1}$, $[\text{CO}] = 1.32 \times 10^{-4} \text{ mol/L}$, $[\text{O}_2] = 20\%$). The photooxidation rates decrease with increasing the concentration of water vapor. In the high concentration region, TiO₂ catalyst shows almost no activity. It has been suggested that water vapor has influence on the rate of the VOC photooxidation with TiO₂ in two ways. It enhances the photooxidation rate by regenerating the OH groups, which are consumed by trapping holes to generate OH radicals.^{44,45} We have reported that water vapor facilitates the decomposition of intermediates on TiO₂ that were formed in the photodecomposition of hydrocarbons.⁴⁶ As a negative effect, it lowers the reaction rate by inhibiting the adsorption of VOCs on catalyst surface.^{38,47} We found that the highest rate for CO photooxidation was obtained when the reaction was carried out without water vapor, and increasing amount of water vapor monotonically decreased the reaction rate. This dependency can be explained by the reaction mechanism in which OH radicals are not the active oxygen species for CO oxidation and adsorption of CO not only on TiO₂ surface but also on Pt is inhibited by water vapor. While water is stabilized on Pt in the form of OH with coadsorbed oxygen,⁴⁸ the presence of water has been reported to inhibit

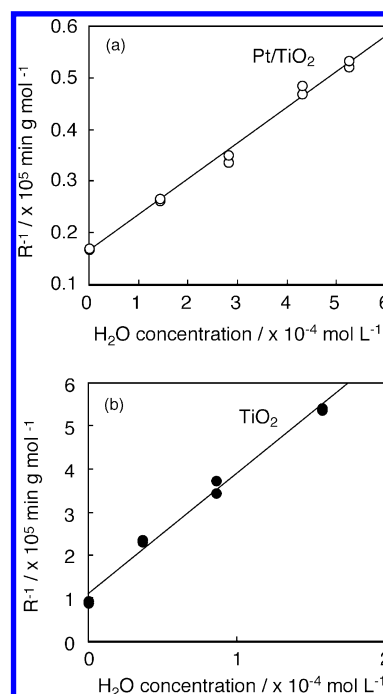


Figure 8. Reciprocal plots of the CO photooxidation over TiO₂ and Pt/TiO₂ versus the concentration of water vapor.

the CO adsorption on Pt.⁴⁹ Therefore, the decrease of rate by the presence of water vapor is explained in terms of the inhibited adsorption of the substrate by water vapor. Assuming that CO and water vapor compete with one another for a limited number of active sites, the reaction rates can be expressed by eqs 10 and 11, where $K_{\text{TiO}_2}^{\text{in}}$ and $K_{\text{Pt}}^{\text{in}}$ are the equilibrium constants for adsorption of water vapor onto TiO₂ and Pt, respectively.^{38,41,50}

$$R = \frac{k_{\text{TiO}_2} K_{\text{TiO}_2} [\text{CO}]}{1 + K_{\text{TiO}_2} [\text{CO}] + K_{\text{TiO}_2}^{\text{in}} [\text{H}_2\text{O}]} \quad (10)$$

$$R = \frac{k_{\text{TiO}_2} K_{\text{TiO}_2} [\text{CO}]}{1 + K_{\text{TiO}_2} [\text{CO}] + K_{\text{TiO}_2}^{\text{in}} [\text{H}_2\text{O}]} + \frac{k_{\text{Pt}} K_{\text{Pt}} [\text{CO}]}{1 + K_{\text{Pt}} [\text{CO}] + K_{\text{Pt}}^{\text{in}} [\text{H}_2\text{O}]} \quad (11)$$

Figure 8 shows the linear correlations for the reciprocals of reaction rates vs the concentrations of water vapor. From the reciprocal plots, numerical values are obtained and compared in Table 1. The reaction rates calculated from the numerical value agree with the experimental data (Figure 7). The equilibrium constant K_{Pt} is twice larger than $K_{\text{Pt}}^{\text{in}}$, while $K_{\text{TiO}_2}^{\text{in}}$ is 13 times larger than K_{TiO_2} . This implies that water vapor is more efficiently adsorbed on the TiO₂ surface than CO, while CO is more efficiently adsorbed on the Pt sites than water vapor. According to the estimation using the calculated data, 32% of active sites on Pt are covered by CO in the $5.22 \times 10^{-4} \text{ mol/L}$ of water vapor (the highest concentration of water vapor in Figure 8). Thus, the kinetic analysis implies that the CO adsorption on Pt is not completely inhibited by larger amount

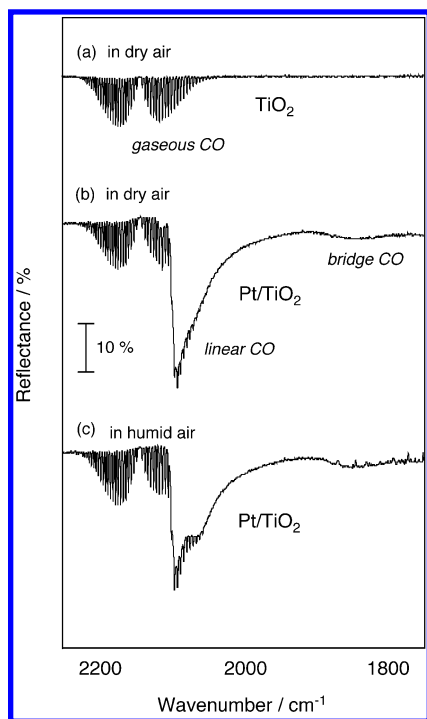


Figure 9. Diffuse reflectance FTIR spectra of CO species during the photoirradiation in air. The spectrum was taken with TiO₂ in the absence of water vapor (a), with Pt/TiO₂ in the absence of water vapor (b), and with Pt/TiO₂ in the presence of water vapor (c). CO concentration: 2.03×10^{-5} mol/L.

of water vapor. It is plausible that the adsorption of CO onto TiO₂ surface is almost completely inhibited in the high concentration of water vapor, and hence, CO photooxidation does not proceed on TiO₂.

Adsorption Behavior of CO on Pt/TiO₂ during the CO Photoreaction. In the kinetic studies described above, it is suggested that CO is efficiently adsorbed on Pt sites. The behavior of CO adsorbed on the catalyst was analyzed by diffuse reflectance FTIR spectroscopy. Figure 9 shows the spectra of CO during the photooxidation over TiO₂ and Pt/TiO₂ catalysts. The spectra were obtained with the resolution of 0.5 cm⁻¹. In the photooxidation with TiO₂, the bands attributable to gaseous CO are observed in the wavenumber region of 2000–2260 cm⁻¹ with the fine structure due to rotational transitions (Figure 9a). For the Pt/TiO₂ catalyst, new absorption bands are observed in the region of 1770–2120 cm⁻¹ with the peaks at 2092 and 1837 cm⁻¹, which are overlapped with the bands of gaseous CO. The fine structure is not observed for the new bands. The disappearance of the fine structure is ascribed to the formation of chemical bonding between the adsorbed CO and Pt metals.⁵¹ These findings indicate that CO is chemically adsorbed on Pt metals during the photooxidation with Pt/TiO₂. The adsorbed CO can be classified into two types of species depending on the coordination states.⁵² The absorption band in the higher region (1910–2120 cm⁻¹) can be assigned to CO linearly coordinated to Pt (abbreviated as linear CO) and that at lower region (1770–1910 cm⁻¹) to CO bridge coordinated to Pt (bridge CO).

The kinetic studies suggest that the adsorption of CO on the active sites on Pt/TiO₂ catalyst is not so much inhibited by water vapor, while that on TiO₂ catalyst is completely inhibited. Figure 9c shows the spectrum obtained when water vapor was coadsorbed on the samples ([H₂O] = 7.0×10^{-4} mol L⁻¹). The chemically adsorbed CO on the Pt metals remains under the humid conditions, although the intensity decreases for the band

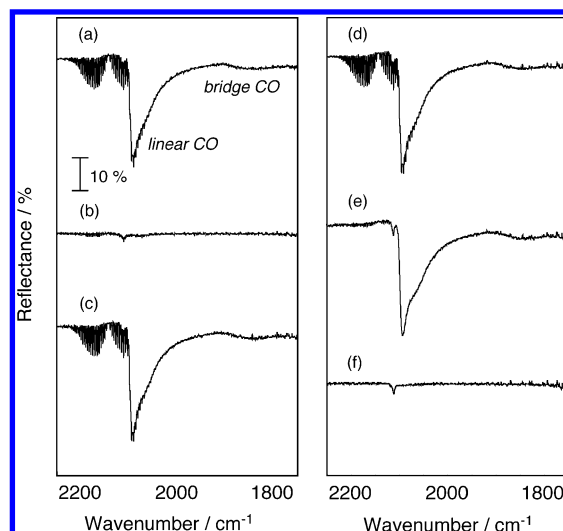


Figure 10. Diffuse reflectance FTIR spectra of CO species on Pt/TiO₂. The spectra a–c were taken with the irradiation in air: (a) with CO; (b) without CO; (c) with CO. The spectrum d was taken with the photoirradiation in the presence of CO. The spectra e and f were taken when the irradiation was stopped and the gas flow was changed to N₂: (e) after 12 min; (f) 16 min.

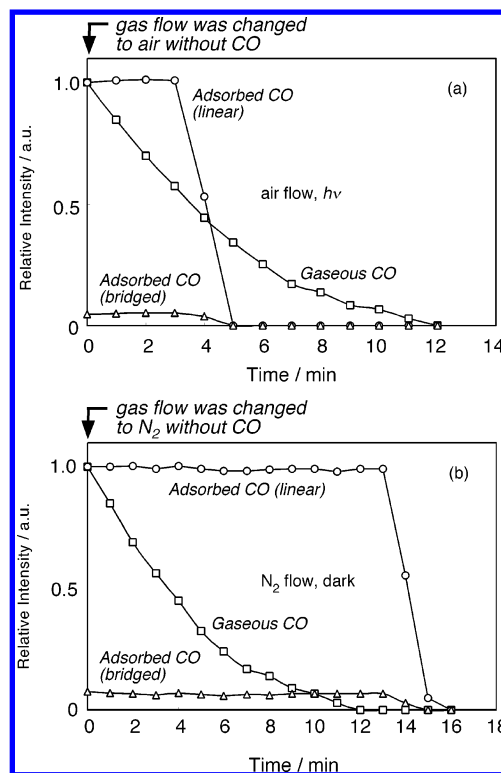


Figure 11. Time course for the change of relative intensity in the bands of adsorbed CO species on Pt sites (2092, 1837 cm⁻¹) and gaseous CO after the CO photooxidation: (a) with photoirradiation in air; (b) without photoirradiation in N₂ flow.

of linear CO. On the other hand, the band of bridge CO is not almost influenced by the presence of water vapor.

After the CO photooxidation with Pt/TiO₂ in air without water vapor (gas flow rate = 500 mL min⁻¹) (Figure 10a), the CO feed was stopped with the continuous photoirradiation. Both linear CO and bridge CO are completely diminished within 5 min, along with the disappearance of gaseous CO (Figure 10b). Thus, these adsorbed CO species desorbed from the catalyst surface. Figure 11a shows the time course for the disappearance of adsorbed CO in this photodesorption process. In the initial

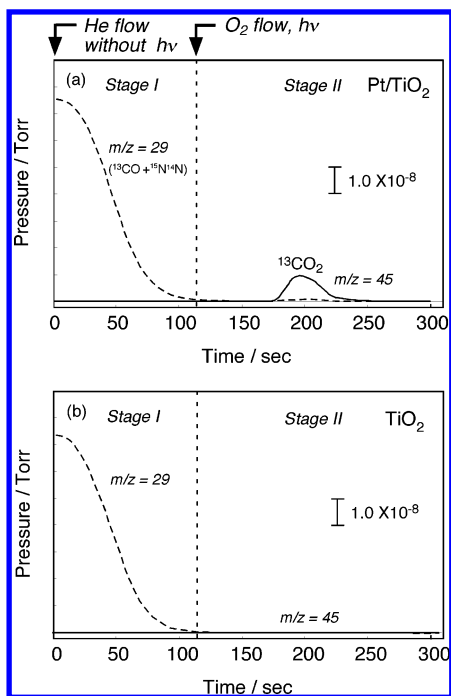


Figure 12. Photodesorption of CO adsorbed on catalyst surface after the catalyst sample was contacted with ^{13}CO in N_2 gas: (a) Pt/TiO_2 ; (b) TiO_2 . The carrier gas was changed from ^{13}CO in N_2 to He without photoirradiation (stage I) and subsequently switched to O_2 flow with photoirradiation (stage II).

period (until 3 min), no changes are observed in the intensity at 2092 cm^{-1} for linear CO or in that at 1837 cm^{-1} for bridge CO. It is likely that the adsorption of CO on Pt and its desorption simultaneously proceeded in this period. After 40% of gaseous CO was removed from the cell, the intensity of the bands due to linear CO and that due to bridge CO immediately decreased, indicating that almost all of the CO desorbed. When the adsorbed CO completely desorbed, the gas flow was switched to the dry air containing $2.03 \times 10^{-5}\text{ mol/L}$ of CO. Figure 10c clearly shows that the band of linear CO and that of bridge CO appear again along with that of gaseous CO. The intensities of these two bands are comparable to those in Figure 10a. Thus, these data clearly show that the adsorption and desorption of CO on the Pt sites reversibly proceed.

Subsequently, the CO photodesorption was carried out in N_2 flow to investigate the effect of O_2 on the desorption behavior of CO on Pt. After the CO photooxidation in air, the photoirradiation was stopped and the gas flow was switched to N_2 without photoirradiation (Figures 10d–f and 11b). The gaseous CO was completely purged from the cell after 12 min. On the other hand, it took about 16 min before the chemically adsorbed CO species completely desorbed from Pt sites. Thus, CO remains on Pt sites even after gaseous CO is completely removed, when O_2 is absent in the reaction gas.

Photodesorption of Adsorbed CO on Pt/TiO_2 . Figure 12 shows the desorption behavior of adsorbed CO on catalyst surface. Prior to the photodesorption measurement, catalyst samples were contacted with the flow of 600 ppm of ^{13}CO in N_2 until adsorption–desorption equilibrium of CO was achieved. Subsequently, the gas flow was switched to He (Figure 12, stage I). As described above, the chemically adsorbed CO on Pt/TiO_2 catalyst remains even after gaseous CO is completely purged from the reactor when O_2 is absent in the reaction gas. After the gaseous CO was purged from the reactor (after 165 s), the gas flow was switched to O_2 with the continuous photoirradiation (Figure 12, stage II). In this stage, $^{13}\text{CO}_2$ was evolved into

the gaseous phase showing that the chemically adsorbed ^{13}CO on Pt metal was oxidized to $^{13}\text{CO}_2$ by the photoirradiation in the presence of O_2 . When the CO desorption measurements were carried out with TiO_2 catalyst, neither $^{13}\text{CO}_2$ nor ^{13}CO was evolved (Figure 12b). These findings support the observations from the FTIR studies that CO is chemically adsorbed only on Pt metals and not on TiO_2 surface.

According to the photodesorption behavior of CO, the amount of $^{13}\text{CO}_2$ evolved from the Pt/TiO_2 catalyst was estimated to be $1.04\text{ }\mu\text{mol}$. As described above, the size of Pt particles was evaluated to be around 2 nm in diameter from the results of TEM and EXAFS. A Pt particle contains 147 atoms and has 92 atoms on its surface, assuming that the particles are the three-shell clusters with fcc structures (particle diameter: 1.95 nm).^{53,54} On the Pt/TiO_2 catalyst used for the CO photodesorption measurement, the total amount of Pt atoms was $2.69\text{ }\mu\text{mol}$ and the amount of Pt atoms on their surface site was $1.68\text{ }\mu\text{mol}$. Therefore, the amount of Pt metals on which CO can be adsorbed is comparable with that of $^{13}\text{CO}_2$ photodesorbed from Pt/TiO_2 catalyst ($1.04\text{ }\mu\text{mol}$), considering that some of the planes on the Pt particles contact with TiO_2 surface⁵⁵ and cannot adsorb CO molecules.

Role of Pt in the Enhanced CO Photooxidation Rate. FTIR studies and CO photodesorption measurements showed that the CO oxidation sites were generated on TiO_2 catalyst by Pt deposition. The adsorption of CO and its desorption on Pt sites reversibly proceed. The adsorbed CO on Pt sites is photooxidized to CO_2 in the presence of O_2 . The reaction rate is expressed as Langmuir–Hinshelwood kinetics that CO is photooxidized to CO_2 both on TiO_2 surface and Pt particles. On the 1.0 wt % of Pt-loaded TiO_2 , 1.5% of TiO_2 surface is covered with Pt metals from the size of Pt particles (2.0 nm) and the surface area of TiO_2 ($43\text{ m}^2/\text{g}$). Instead, approximately 1.2×10^{19} of active sites are newly generated on the 1.0 g of TiO_2 surface, according to the results from CO photodesorption measurements.

The adsorption of CO on the catalyst surface is one of the key steps in the photocatalyzed CO oxidation. Deposition of Pt on TiO_2 generates the active sites on which CO is chemically coordinated. Kinetic analysis indicates that, in the CO photooxidation on Pt/TiO_2 surface, CO is efficiently adsorbed on Pt sites as compared with TiO_2 surface. This mechanism can also account for the effect of water vapor on the reaction rates. Water vapor decreases the CO photooxidation rate, since it inhibits the adsorption of CO on active sites. CO photooxidation hardly proceeds on the TiO_2 surface in the presence of water vapor, probably because CO adsorption on TiO_2 is completely suppressed. On the other hand, the adsorption of CO on Pt is not so much inhibited by the presence of water vapor, and the reaction proceeds even in the high concentration of water vapor. The kinetic analysis also implies that the rate for the oxidation of adsorbed CO to CO_2 on Pt sites is larger than that on TiO_2 surface. The surface site density on TiO_2 is estimated to be $(3.0\text{--}4.2) \times 10^{20}\text{ sites/g}$ of Pt/TiO_2 according to the specific surface area of TiO_2 ($43\text{ m}^2/\text{g}$), the area of TiO_2 covered with Pt, and the cation site density of anatase or rutile $((7\text{--}10) \times 10^{18}\text{ sites/m}^2)$. The kinetic constant/active site is $4.70 \times 10^{-24}\text{ mol min}^{-1}(\text{site})^{-1}$ for Pt and is about 40–60 times larger than that for TiO_2 $((0.76\text{--}1.06) \times 10^{-25}\text{ mol min}^{-1}(\text{site})^{-1})$. Thus, the reaction rate constant/site is much larger for Pt than for Ti.

According to our previous data on ESR measurements, the active oxygen species O^- and O_3^- are formed on the photooxidation on Pt/TiO_2 and they oxidize CO to CO_2 .³⁶ As shown in FTIR studies, the presence of O_2 facilitates the desorption of

CO on Pt. This indicates that O₂ plays the important role in the CO photooxidation. However, the investigation of its role is beyond the scope of this paper and will be described elsewhere.

Conclusions

In this study, Pt-deposited TiO₂ catalysts with 2–3 nm of Pt particles were prepared by photodeposition method and tested for the CO photooxidation at room temperature. Pt/TiO₂ catalyst showed higher activity than TiO₂ catalyst. The reaction rate increased with light intensity to the power of 0.5 and 0.7 for TiO₂ and Pt deposited TiO₂ catalysts, respectively. The dependencies of reaction rate on the concentration of CO and water vapor were explained in terms of the Langmuir–Hinshelwood type mechanism, where CO was photooxidized both on TiO₂ and Pt particles and water vapor inhibited the CO adsorption. Kinetic parameters imply that CO is efficiently adsorbed on Pt sites and its adsorption is not so much inhibited by water vapor as compared with the TiO₂ surface. Diffuse reflectance FTIR spectra showed that CO was chemically adsorbed on the Pt metals with two types of bonding, that is, linearly coordinated CO and bridge coordinated CO. The adsorption and desorption of CO reversibly proceeded for both types of bonding. The adsorbed CO on Pt was oxidized to CO₂ by photoirradiation in the presence of O₂. The amount of CO evolved was comparable with that of Pt atoms on their surface site. According to these findings, we conclude that the role of Pt metals on TiO₂ is to generate the active sites on which CO is efficiently adsorbed and oxidized to CO₂.

Acknowledgment. This work was financially supported by Industrial Technology Research Grant Program '00 from the New Energy and Industrial Technology Development Organization of Japan (NEDO).

References and Notes

- (1) Fu, X.; Zeltner, W. A.; Anderson, M. A. In *Semiconductor Nanoclusters-Physical, Chemical, and Catalytic Aspects*; Kamat, P. V., Meisel, D., Eds.; Elsevier Science Publishers: Amsterdam, 1996; p 445.
- (2) Hoffmann, M. R.; Martin, S. T.; Choi, W.; Bahnemann, D. W. *Chem. Rev.* **1995**, 95, 69.
- (3) Linsebigler, A. L.; Lu, G.; Yates, J. T., Jr. *Chem. Rev.* **1995**, 95, 735.
- (4) Fox, M. A.; Dulay, M. T. *Chem. Rev.* **1993**, 93, 69.
- (5) Mills, A.; Davies, R. H.; Worsley, D. *Chem. Soc. Rev.* **1993**, 22, 417.
- (6) Howe, R. F.; Gratzel, M. *J. Phys. Chem.* **1987**, 91, 3906.
- (7) Naccache, C.; Meriaudeau, P.; Che, M.; Tench, A. J. *Trans. Faraday Soc.* **1971**, 67, 506.
- (8) Gerisher, H. *J. Phys. Chem.* **1984**, 88, 6096.
- (9) Ohtani, B.; Bowman, R. M.; Colombo, D. P.; Kominami, H.; Noguchi, H.; Uosaki, K. *Chem. Lett.* **1998**, 579.
- (10) Sato, S.; White, J. M. *Chem. Phys. Lett.* **1980**, 72, 83.
- (11) Sato, S.; White, J. M. *J. Phys. Chem.* **1981**, 85, 592.
- (12) Kawai, T.; Sakata, T. *J. Chem. Soc., Chem. Commun.* **1980**, 694.
- (13) Pichat, P.; Herrmann, J.-M.; Disdier, J.; Courbon, H.; Mozzanega, M.-N. *Nouv. J. Chim.* **1981**, 5, 627.
- (14) Izumi, I.; Fan, F.-R. F.; Bard, A. J. *J. Phys. Chem.* **1981**, 85, 218.
- (15) St. John, M. R.; Furgala, A. J.; Sammells, A. F. *J. Phys. Chem.* **1983**, 87, 801.
- (16) Izumi, I.; Dunn, W. W.; Wilbourn, K. O.; Fan, F.-R. F.; Bard, A. J. *J. Phys. Chem.* **1980**, 84, 3207.
- (17) Jaffrezic-Renault, N.; Pichat, P.; Foissy, A.; Mercier, R. *J. Phys. Chem.* **1986**, 90, 2733.
- (18) Einaga, H.; Futamura, S.; Ibusuki, T. *Environ. Sci. Technol.* **2001**, 35, 1880.

- (19) Vorontsov, A. V.; Savinov, E. N.; Barannik, G. B.; Troitsky, V. N.; Parmon, V. N. *Catal. Today* **1997**, 39, 207.
- (20) Takahama, K.; Sako, T.; Yokoyama, M.; Hirao, S. *Nippon Kagaku Kaishi* **1994**, 7, 613.
- (21) Linsebigler, A.; Rusu, C.; Yates, J. T., Jr. *J. Am. Chem. Soc.* **1996**, 118, 5284.
- (22) Engel, T.; Ertl, G. *Adv. Catal.* **1979**, 28, 1.
- (23) Kenned, J. C., III; Datye, A. K. *J. Catal.* **1998**, 179, 375.
- (24) Teo, B. K. *EXAFS Basic Principles and Data Analysis, Inorganic Chemistry Concepts*; Springer-Verlag: Berlin, 1986; Vol. 9.
- (25) Koningsberger, D. C.; Prins, R. *X-ray Absorption: Principles, Applications, Techniques of EXAFS, SEXAFS, and XANES*; John Wiley & Sons: New York, 1988.
- (26) Murov, S. L. *Handbook of Photochemistry*; Marcel Dekker: New York, 1974.
- (27) Jacoby, W. A.; Blake, D. M.; Noble, R. D.; Koval, C. A. *J. Catal.* **1995**, 157, 87.
- (28) Einaga, H.; Futamura, S.; Ibusuki, T. *Phys. Chem. Chem. Phys.* **1999**, 1, 4903.
- (29) Ohko, Y.; Hashimoto, K.; Fijishima, A. *J. Phys. Chem. A* **1997**, 101, 8059.
- (30) Aguad, M. A.; Anderson, M. A.; Hill, C. G., Jr. *J. Mol. Catal.* **1994**, 89, 165.
- (31) D'Oliveira, J.-C.; Al-Sayyed, G.; Pichat, P. *Environ. Sci. Technol.* **1990**, 24, 990.
- (32) Kormann, C.; Bahnemann, D. W.; Hoffmann, M. R. *Environ. Sci. Technol.* **1991**, 25, 494.
- (33) Hoffman, A. J.; Carraway, E. R.; Hoffmann, M. R. *Environ. Sci. Technol.* **1994**, 28, 776.
- (34) When α for Pt/TiO₂ is a convolution of α for TiO₂ (denoted by α_1) and that for Pt (α_2), the equation may be described as follows on the condition that the same reaction process is involved in the CO oxidation on Pt as on TiO₂: $R = k_1 I^{\alpha_1}$ (for TiO₂); $R = k_1 I^{\alpha_1} + k_2 I^{\alpha_2}$ (for Pt/TiO₂). If the value α_1 is assumed to be unchanged by Pt deposition, the values are estimated to be 0.7 for α_1 and 0.4 for α_2 , respectively.
- (35) Egerton, T. A.; King, C. J. *J. Oil. Colour Chem. Assoc.* **1979**, 62, 386.
- (36) We have suggested that this phenomenon is ascribed to the stabilization of active oxygen species O⁻ and O₃⁻ on Pt/TiO₂: Einaga, H.; Ogata, A.; Futamura, S.; Ibusuki, T. *Chem. Phys. Lett.* **2001**, 338, 303.
- (37) Baddour, R. F.; Modell, M.; Heusser, U. K. *J. Phys. Chem.* **1968**, 72, 3621.
- (38) Dibble, L. A.; Raupp, G. B. *Catal. Lett.* **1990**, 4, 345.
- (39) Pruden, A. L.; Ollis, D. F. *J. Catal.* **1983**, 82, 404.
- (40) Al-Ekabi, H.; Serpone, N. *J. Phys. Chem.* **1988**, 92, 5726.
- (41) Zorn, M. E.; Tompkins, D. T.; Zeltner, W. A.; Anderson, M. A. *Appl. Catal., B: Environ.* **1999**, 23, 1.
- (42) In this study, the O₂ concentration is fixed for the kinetic analysis, and we assumed that the fractional coverage of oxygen is unchanged by the CO concentration. By this treatment, the rate can be expressed in the form of eqs 6 and 7.
- (43) The plots in Figures 6 and 8 were fitted with straight lines by the least-squares method. Kinetic parameters were estimated by the approximation that the kinetic constants K_{TiO_2} , k_{TiO_2} , and $K_{\text{TiO}_2}^{\text{in}}$ were unchanged by Pt deposition.
- (44) Phillips, L. A.; Raupp, G. B. *J. Mol. Catal.* **1992**, 77, 297.
- (45) Cao, L.; Huang, A.; Spiess, F.-J.; Suib, S. L. **1999**, 188, 48.
- (46) Einaga, H.; Futamura, S.; Ibusuki, T., *Appl. Catal., B: Environ.* **2002**, 38, 215.
- (47) Fu, X.; Clark, L. A.; Zeltner, W. A.; Anderson, M. A. *J. Photochem. Photobiol., A: Chem.* **1996**, 97, 181.
- (48) Bedurfing, K.; Volkening, S.; Wang, Y.; Wintterlin, J.; Jacobi, K.; Ertl, G. *J. Chem. Phys.* **1999**, 111, 11147.
- (49) Lofgren, P.; Kasemo, B. *Catal. Lett.* **1998**, 53, 33.
- (50) Luo, Y.; Ollis, D. F. *J. Catal.* **1996**, 163, 1.
- (51) Niemantsverdriet, J. W. *Spectroscopy in Catalysis*; VCH Publishers: New York, 1995.
- (52) Sheppard, N.; Nguyen, T. T. In *Advances in Infrared and Raman Spectroscopy*; Clark, R. J. H., Hester, R., Eds.; Heyden: London, 1978; Vol. 5, p 67.
- (53) See, for example: Clausen, B. S.; Topsøe, H.; Hansen, L. B.; Stoltze, P.; Norskov, J. K. *Jpn. J. Appl. Phys.* **1993**, 32 (Suppl. 32–2), 95.
- (54) Bradley, J. S. In *Clusters and Colloids: From Theory to Applications*; Schmid, G., Ed.; VCH: Weinheim, Germany, 1994; pp 459–544.
- (55) Tsujimoto, M.; Moriguchi, S.; Isoda, S.; Kobayashi, T.; Komatsu, T. *J. Electron Microsc.* **1999**, 48, 361.